SUPPORTING INFORMATION

MODULATING LIPOPROTEIN TRANSCELLULAR TRANSPORT AND ATHEROSCLEROTIC PLAQUE FORMATION IN APOE$^{-/-}$ MICE VIA NANOFORMULATED LIPID-METHOTREXATE CONJUGATES

Valentina Di Francesco[1,2], Danila Gurgone[3,4], Roberto Palomba[1], Miguel Filipe Moreira Marques Ferreira[1], Tiziano Catelani[6], Antonio Cervadoro[1], Pasquale Maffia[3,4,5,♣], Paolo Decuzzi [1, ♣, *]

[1]Laboratory of Nanotechnology for Precision Medicine, Fondazione Istituto Italiano di Tecnologia. Via Morego 30, 16163, Genoa, Italy

[2]Department of Informatics, Bioengineering, Robotics and System Engineering, University of Genoa, Via Opera Pia, 13 Genoa 16145

[3]Centre for Immunobiology, Institute of Infection, Immunity and Inflammation, College of Medical, Veterinary and Life Sciences, University of Glasgow, Glasgow, G12 8TA, United Kingdom

[4]Department of Pharmacy, University of Naples Federico II, Naples, 80131, Italy

[5]Institute of Cardiovascular and Medical Sciences, College of Medical, Veterinary and Life Sciences, University of Glasgow, Glasgow, G12 8TA, United Kingdom

[6]Electron Microscopy Facility, Istituto Italiano di Tecnologia, via Morego 30, Genova, 16163, Italy

♣ Shared senior authorship

* Corresponding Author: Paolo Decuzzi, PhD paolo.decuzzi@iit.it

SUPPLEMENTARY RESULTS

DSPE-MTX prodrug synthesis. Considering the poor solubility of the Methotrexate (MTX), a prodrug with amphiphilic properties was generated by binding MTX to 1,2-distearoyl-sn-glycero-3-phosphoethanolamine-N-amino (DSPE-NH2). In order to generate the prodrug, MTX was pre-activated *in loco* with a mixture of DCC and NHS, then conjugated with DSPE-NH_2. Compound purification was achieved by precipitation in cold diethyl ether.

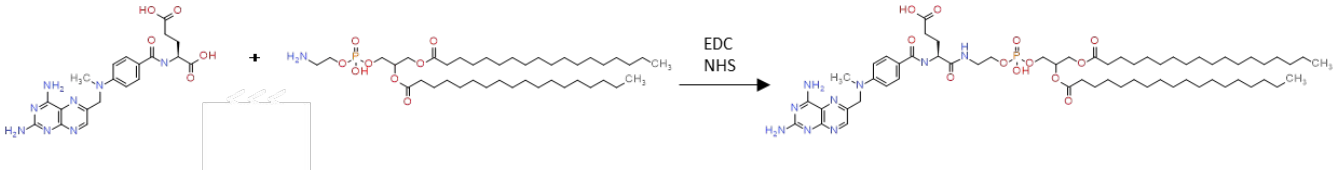

Figure S1. Synthesis of prodrug.

MTX-loaded nanoparticles stability under slightly acidic conditions

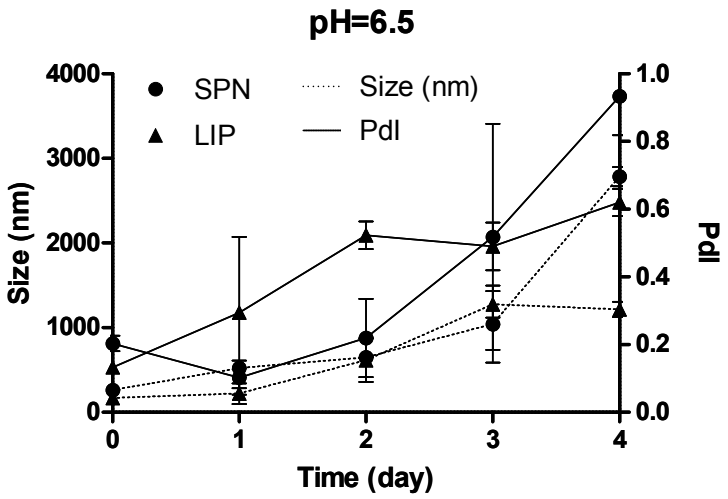

Figure S2. Particle stability at pH=6.5.

MTX-SPN optimization. Optimization of SPN. To find the optimal formulation, MTX-SPNs were produced using different amounts of PLGA and DPPC and using PLGA with different molecular weights (25-35KDa or 38-53KDa) as reported in **Table S1, Figure S3**. To find the optimal formulation, MTX-SPNs were produced using different amounts of PLGA and DPPC and using PLGA with different molecular weights (25-35KDa or 38-53KDa). All the formulations presented average sizes ranging from 200 to 225 nm and showed a negative ζ-potential ranging from - 41 to - 54 mV. With the increase of PLGA amount a relative increase on the nanoparticles size was retrieved. The negative charge is related to DSPE-PEG-COOH carboxylic groups exposed on SPNs surface. As shown in **Figure S3A** and **B** the amount of PLGA also affected DSPE-MTX encapsulation efficiency (EE%) which increases proportionally to PLGA amount, passing from about 0.2% to 0.5 % for the lowest molecular weight PLGA (25-35KDa) and from 0.4% to 1.5% for the highest (38-53kDa). EE% was also affected by the presence of DPPC, by removing DPPC the amount of internalized prodrug increased. This finding is probably related to a competition between DSPE-MTX and DPPC on the stabilization of the PLGA during the addition to the aqueous phase on the preparation of the nanoparticles. Basing on these considerations, SPNs 12 formulation was selected (**Table S1, Figure S3**). Starting from now on, we will refer to SPNs12 as MTX-SPNs.

Table S1: Optimization of SPNs. The SPNs were made in triplicate (n=3) for each single experiment.

Sample	PLGA (23-35 kDa) (mg)	PLGA (38-53 kDa) (mg)	DPPC (mg)	DSPE-MTX (mg)	DSPE-PEG (mg)	Size (nm)	PdI	Z Pot (mV)	Mass of DSPE-MTX (µg)	EE(%)
SPN 1	0.5	-	0.09	0.2	0.11	200±2	0.12±0.02	-52±2.3	0.25±0.025	0.13±0.01
SPN 2	0.5	-	-	0.2	0.11	200±3	0.1±0.02	-46±5	0.26±0.06	0.13±0.03
SPN 3	1	-	0.09	0.2	0.11	201±9	0.13±0.03	-54±1	0.36±0.09	0.18±0.04
SPN 4	1	-	-	0.2	0.11	210±12	0.18±0.02	-44±15	0.52±0.02	0.26±0.01
SPN 5	2	-	0.09	0.2	0.11	223±14	0.18±0.03	-51±2	0.58±0.16	0.29±0.08
SPN 6	2	-	-	0.2	0.11	215±6	0.18±0.02	-48±3.6	0.76±0.09	0.38±0.05
SPN 7	-	0.5	0.09	0.2	0.11	200±2	0.1±0.02	-46.5±0.5	0.26±0.06	0.13±0.03
SPN 8	-	0.5	-	0.2	0.11	202±10	0.13±0.03	-41±1.5	0.41±0.04	0.21±0.02
SPN 9	-	1	0.09	0.2	0.11	215±6	0.18±0.02	-44±1.5	0.52±0.02	0.26±0.01
SPN 10	-	1	-	0.2	0.11	205±7	0.16±0.03	-46±2	0.87±0.2	0.43±0.1
SPN 11	-	2	0.09	0.2	0.11	218±1	0.19±0.02	-48±3.6	0.76±0.09	0.38±0.05
SPN 12	-	2	-	0.2	0.11	208±2	0.15±0.02	-45±0.02	3±0.34	1.5±0.17

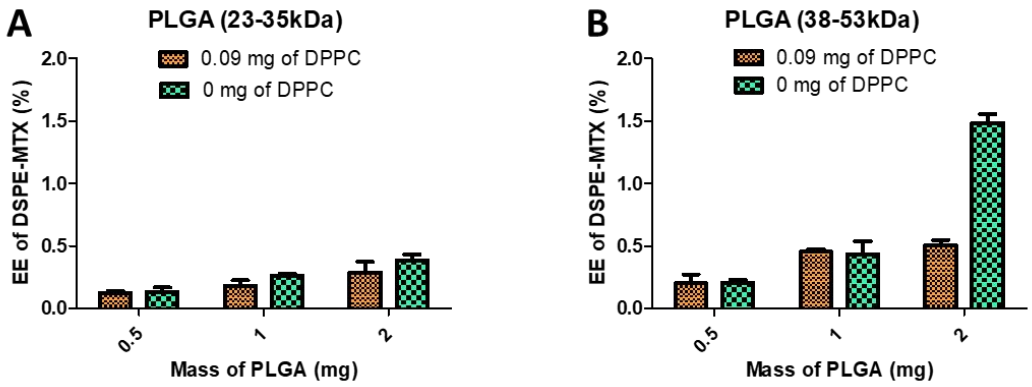

Figure S3: A. and B. Different formulations with different amounts of PLGA and DPPC: EE% of DSPE-MTX.

Oxidized Low Density Lipoproteins (oxLDL)

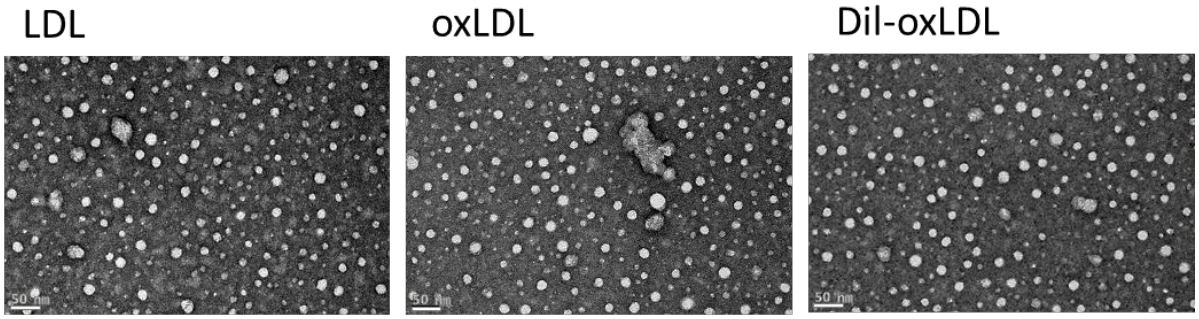

Figure S4. TEM images of LDL molecules (left), oxLDL molecules (center), DiI-oxLDL (right) (scale bar = 50 μm).

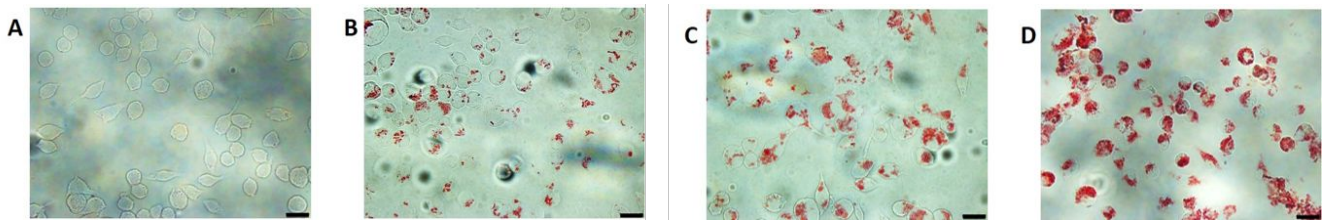

Figure S5. Incubation of oxLDL with macrophages (RAW 264.7). **A.** 0 μg/ml oxLDL; **B**. 20 μg/ml oxLDL; **C**. 50 μg/ml oxLDL; **D**. 80 μg/ml oxLDL (scale bar = 25 μm).

Intracellular localization of oxLDL. To observe oxLDL intracellular distribution at confocal microscopy oxLDL were stained using DiI; for this experiment living RAW 264.7 were treated with 488-lysotracker to highlight lysosomes and with a concentration of DiI-oxLDL equivalent to 50 μg/ml of oxLDL. As it is possible to appreciate the green signal from lysosomes and the red signal from oxLDL co-localize almost completely, proving oxLDL accumulation mainly occurs into lysosomes (**Figure S6A**). Control cells were treated only with DiI (instead of DiI-oxLDL) following the same conditions, as it is possible to observe in **Figure S6B**. No co-localization at lysosomes was observed. Red signal coming from DiI was confined to plasma membrane. It is also important to underline that in cells treated with DiI-oxLDL no fluorescent signal was retrieved at plasma membrane thus proving the absence of any leakage of DiI from fluorescent oxLDL.

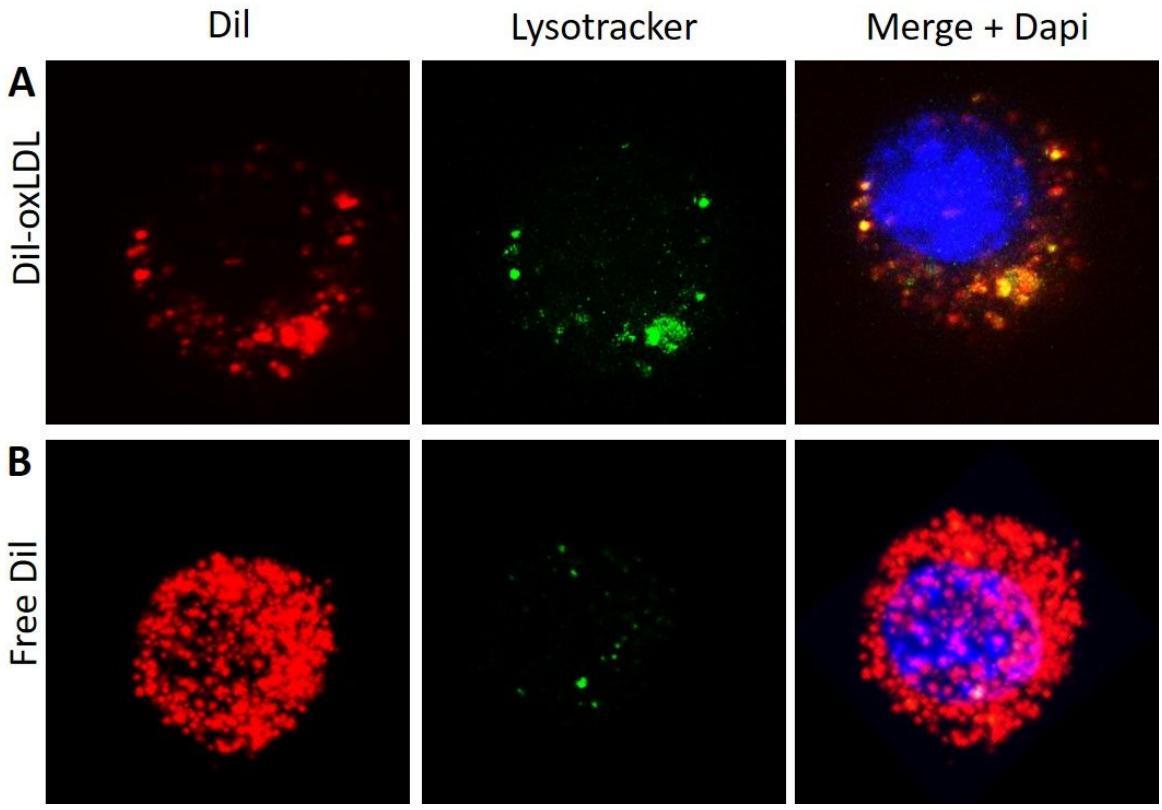

Figure S6. Raw 264.7 cells treated with **A**. Dil-oxLDL and **B**. Free Dil. In red Dil and Dil-oxLDL, in green Lysotracker and in blue DAPI.

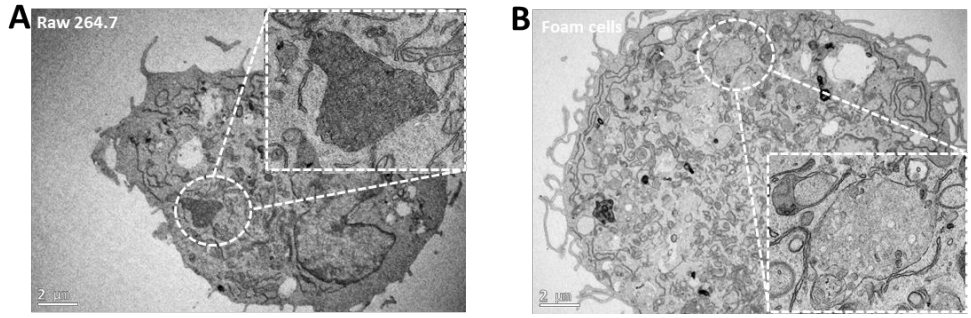

Figure S7 TEM images of macrophages. A. RAW 264.7 cells not exposed to oxLDL show dark lysosomal structures. **B**. RAW 264.7 cells exposed to oxLDL (overnight, 50 μg/ml) show light lysosomal structures due to the high lipid content.

Stable association of DiI and oxLDL molecules. To furtherly demonstrate the stability of oxLDL and DiI a time-lapse microscopy experiment was performed (**Movie S1** and **S2**). Following the same condition living BMDM were incubated overnight with DiI-oxLDL or with DiI. 14 hours after treatment cells were observed at the microscope and movies (**Movie S1**) were recorded. In DiI-oxLDL treated cells it is possible to note particulate movement inside the cell referring to DiI-oxLDL trafficking; in free DiI treated cells, **Movie S2**, instead the fluorescent signal is revealed from firm spots most likely located in plasma membrane.

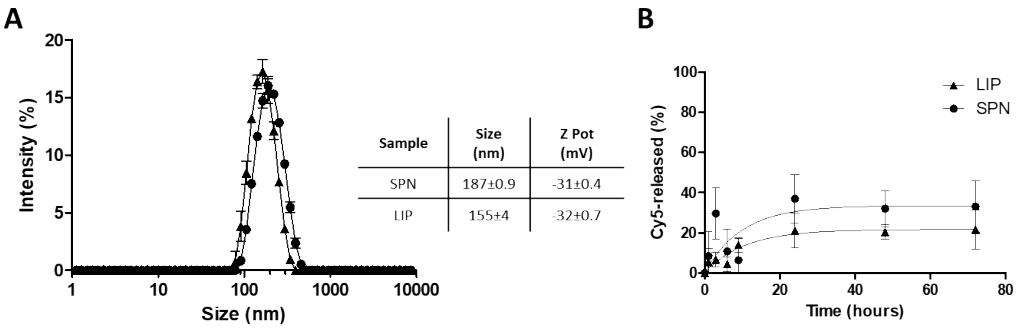

Sample	Size (nm)	Z Pot (mV)
SPN	187±0.9	-31±0.4
LIP	155±4	-32±0.7

Figure S8 A. DLS analysis of Cy5-LIP and Cy5-SPN. **B.** Release study of Cy5 from LIP and SPN.

Expression levels for the genes regulating the cholesterol transport

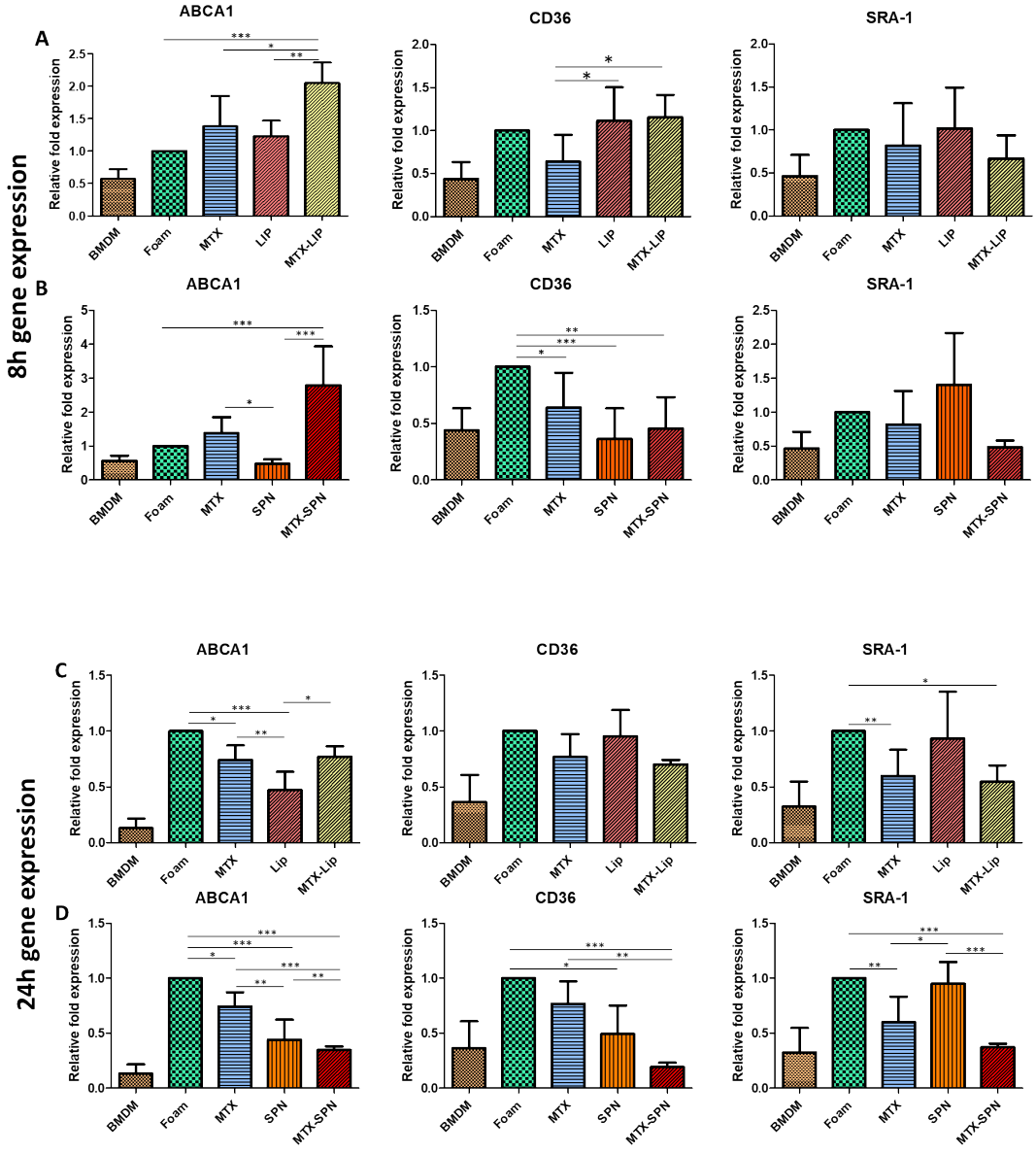

Figure S9 A-D. Foam cells markers expression level (ABCA1, CD36, and SR-A1) in foam cells (treated for 8 and 24 hours with the free and empty/loaded drug in LIP and SPN). Results are expressed as average ± SD (n = 5). ***p < 0.0001; **p < 0.001; *p < 0.01

Expression levels for the genes associated with the anti-inflammatory cytokines

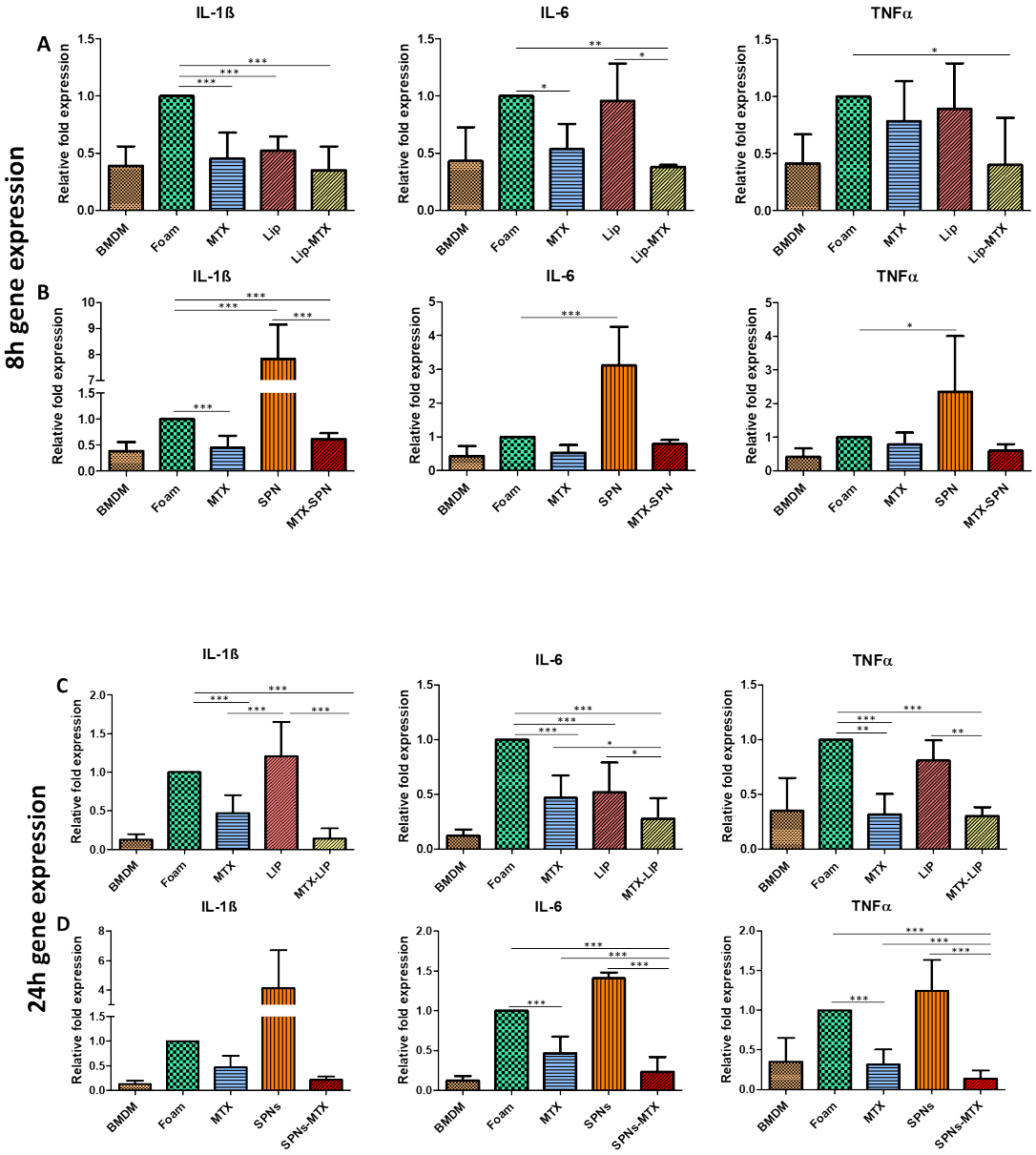

Figure S10 A-D. Pro-inflammatory cytokines expression levels (TNF-α, IL-1β, and IL-6) in foam cells (treated for 8 and 24 hours with the free and empty/loaded drug in LIP and SPN). Results are expressed as average ± SD (n = 5). ***p < 0.0001; **p < 0.001; *p < 0.01

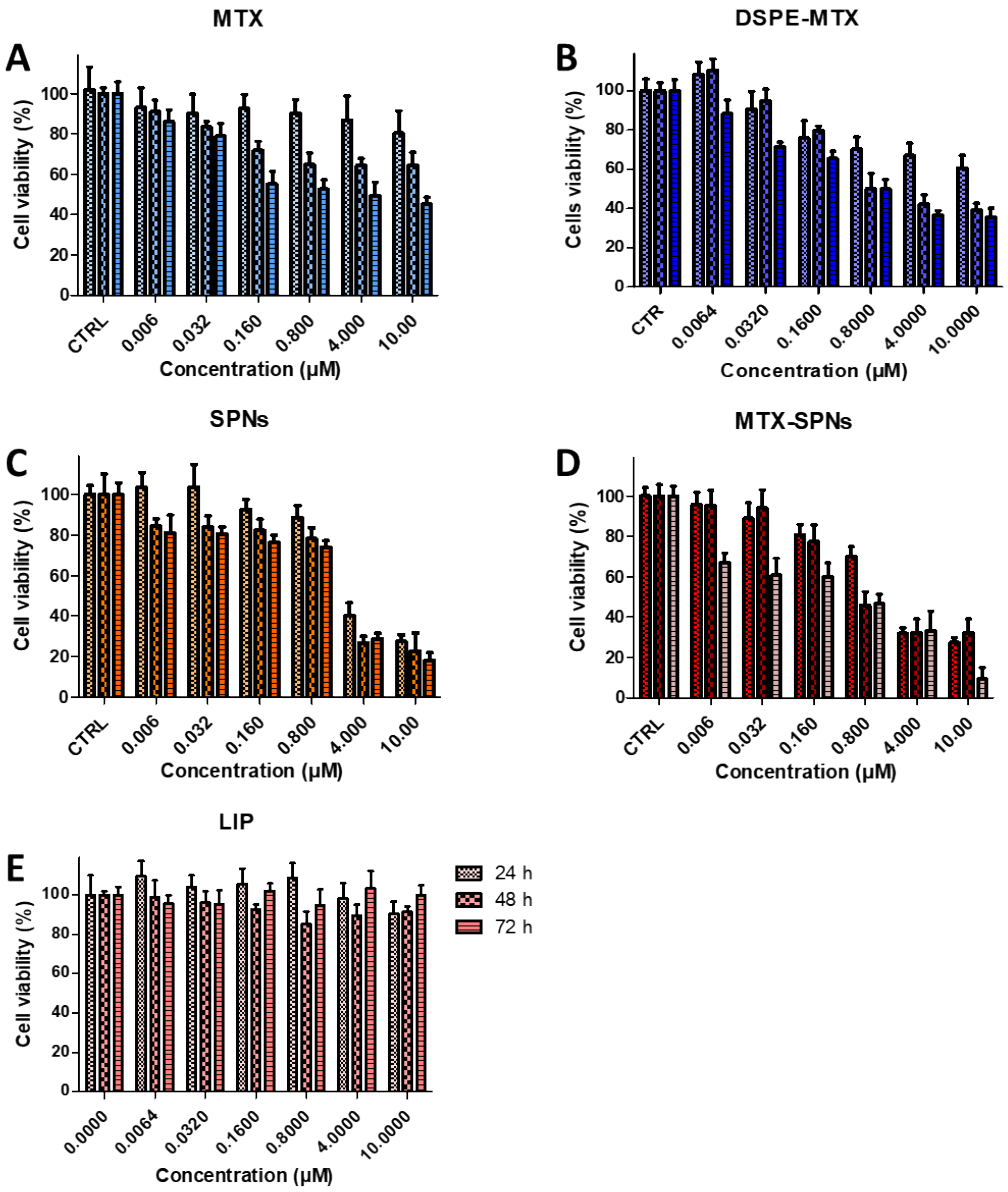

Figure S11 A-E. Viability of BMDM incubated with MTX, DSPE-MTX, empty SPN, MTX-SPN and empty LIP a 3 different time points.

Table S2 Luminex results.

Cytokine (pg/ml)	LIP	MTX-LIP
IL-1α	7.7±1	11.1±1.2
IL-1β	-	-
IL-2	-	-
IL-3	7.3±0.67	8.13±0.67
IL-4	2.6±0.2	2.4±0.3
IL-5	7±0.8	10.1±1.1
IL-6	11.7±3	13.6±3.75
IL-9	41.3±6.3	40.6±3.3
IL-12p40	970.8±68	930.5±72
IL-12p70	2263±98	2541.9±
IL-13	82.2±13	89±8.2
IL-17A	189.9±28	227.4±18.5
Eotaxin	2084.3±210	1866.3±160
G-CSF	308.6±85	419.6±129.5
GM-CSF	-	-
IFN-Ɣ	43.8±3.4	43.8±4.9
KC	58±8.9	53.3±10
MCP-1	257.8±31.6	265.5±26.6
MIP-1α	6.2±0.2	6.29±0.4
MIP-1β	25.8±1.7	25.2±1.36
RANTES	68.6±8.44	51.84±6.6
TNF-α	1386.2±60.7	1493±108

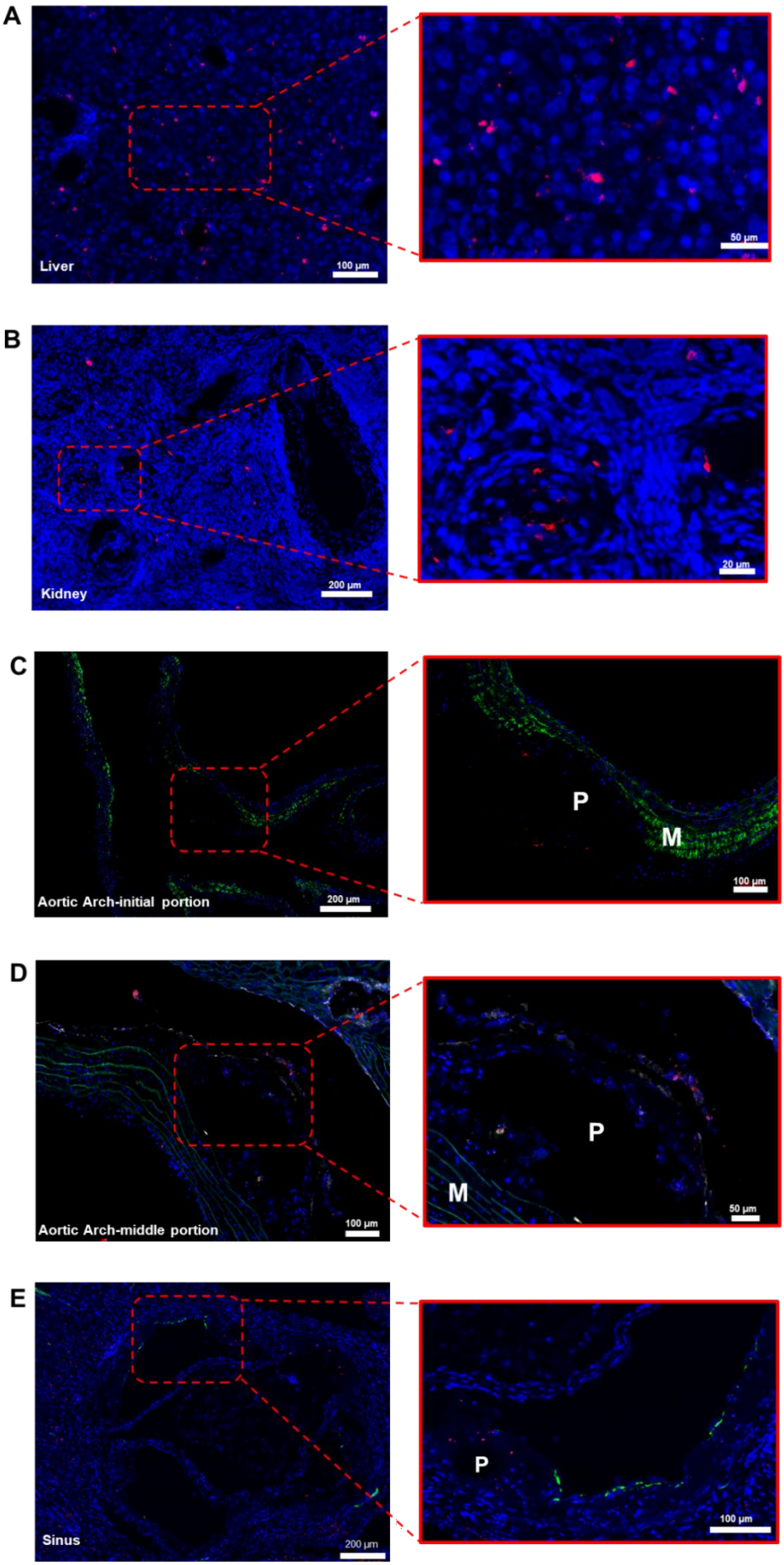
A
Liver
100 μm
50 μm
B
Kidney
200 μm
20 μm
C
Aortic Arch-initial portion
200 μm
P
M
100 μm
D
Aortic Arch-middle portion
100 μm
P
M
50 μm
E
Sinus
200 μm
P
100 μm

Figure S12 Representative Bio-distribution confocal imaging after injection of Cy5-liposomes (red signal) in a one-year-old female apoE$^{-/-}$ mouse. Liver (**A**), and kidney (**B**), aortic arch: initial portion (**C**), middle portion (**D**) and aortic sinus (**C**). In **C** and **D** α-smooth muscle actin (α-SMA) was stained by immunofluorescence (green signal), in all of the images cell nuclei were stained using DAPI (blue signal). Insets: M= Media; P= Plaque.

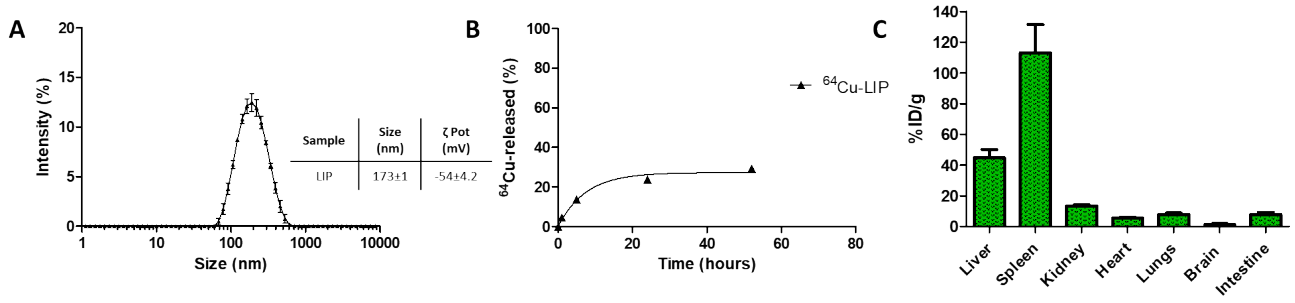

Figure S13 Bio-distribution study. **A.** DLS analysis of ^{64}Cu-LIP. **B**. Release study of ^{64}Cu from LIP. **C.** Quantitative assessment of radioactivity distribution in selected tissues 24 h after injection (n = 5).

SUPPLEMENTARY MOVIES

Movie S1: Trafficking of Dil-oxLDL.

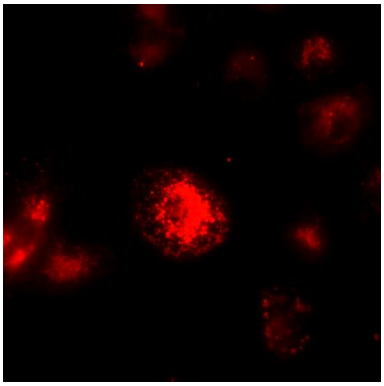

Foam: BMDM + Dil-oxLDL for 14h

Movie S2: Cellular membrane staining.

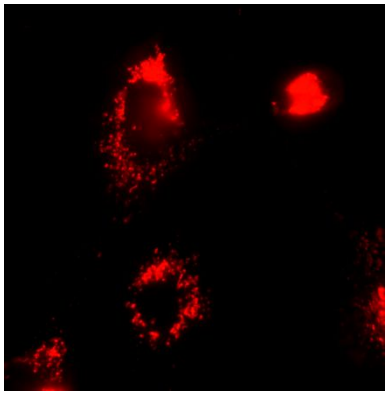

BMDM + Dil for 14h